Available online at www.sciencedirect.com
ScienceDirect
Journal of Magnetism and Magnetic Materials 319 (2007) 64–68
Journal of magnetism and magnetic materials
www.elsevier.com/locate/jmmm

# Magnetic, and electronic properties of a $Ba_3InRu_2O_9$ single crystal

L. Shlyk[a,*], S. Kryukov[a], V. Durairaj[a], S. Parkin[b], G. Cao[a], L.E. De Long[a]

[a] University of Kentucky, Department Physics and Astronomy, Lexington, KY 40506, USA
[b] University of Kentucky, Department Chemistry, Lexington, KY 40506, USA

Received 11 December 2006; received in revised form 20 April 2007
Available online 8 May 2007

**Abstract**

The magnetic and transport properties of a $Ba_3InRu_2O_9$ single crystal are reported. $Ba_3InRu_2O_9$ crystallizes in a hexagonal $BaTiO_3$ structure, consisting of face-sharing $RuO_6$ octahedra interconnected by corner-sharing $InO_6$ octahedra. The $Ru_2^{4.5+}O_9$ dimers form $S = \frac{1}{2}$ spins on a distorted hexagonal lattice that frustrates antiferromagnetic interdimer interactions and results in a spin-glass transition at $T_g = 3.5$ K. The compound is a semiconductor that exhibits variable-range hopping as the transport mechanism in the temperature range 140–600 K.


*PACS:* 74.70.Pq; 75.10.Nr

*Keywords:* Ruthenate; Spin glass; Magnetic properties

## 1. Introduction

Transition metal oxides continue to attract great attention in physics and materials chemistry. In particular, ruthenium oxides have been actively investigated, primarily because they exhibit a wide variety of unusual magnetic and electronic properties. Obvious examples are the exotic superconductor $Sr_2RuO_4$ ($T_s = 1$ K [1]), the metallic ferromagnet $SrRuO_3$ ($T_c = 160$ K [2]), $Sr_3Ru_2O_7$ (paramagnetic close to a quantum critical state [3]), and the "borderline metamagnet" $Sr_4Ru_3O_{10}$ [4]. In this paper, we examine the electrical and magnetic properties of a $Ba_3InRu_2O_9$ single crystal, which is a member of a large family of ruthenium oxides with the general formula $Ba_3MRu_2O_9$, where M is a transition [5,6] or lanthanide element [7].

Overall charge balance of the formula units dictates a mixed valence state of $Ru^{4+}$ and $Ru^{5+}$ for the composition of $Ba_3MRu_2O_9$. This material crystallizes in the 6H-perovskite structure, in which Ru occupies the face-sharing octahedral sites forming $Ru_2^{4.5+}O_9$ dimers, interconnected by corner sharing with $MO_6$ octahedra. The Ru–Ru distances within the dimers are short (2.48–2.69 Å), which signals strong magnetic interactions. On the other hand, the interdimer distances are much larger, indicating that the coupling between the dimers is weak enough to support covalent bonding within the dimers, which leads to semiconducting behavior of this material.

To our knowledge, structural, magnetic and resistivity data are available only for polycrystalline samples of this series of compounds, and certain inconsistencies in the magnetic data have been published for $Ba_3InRu_2O_9$. In Ref. [5], the susceptibility of this compound is reported to be nearly equal to that of $BaRuO_3$, showing only weakly temperature-dependent paramagnetic behavior below 400 K. On the other hand, Doi et al. [8] report that the susceptibility of polycrystalline $Ba_3InRu_2O_9$ shows complex magnetic properties that include two anomalies, i.e., a broad maximum at 370 K and another magnetic anomaly at 4.5 K. The high-temperature anomaly is attributed to an antiferromagnetic coupling between two Ru ions in a $Ru_2^{4.5+}O_9$ dimer, while the peak at low temperature is related to antiferromagnetic interactions between the $Ru_2^{4.5+}O_9$ dimers. In order to get further insight about the magnetic interactions within and between the $Ru_2^{4.5+}O_9$ dimers, we have re-examined the magnetic and transport

*Corresponding author. Tel.: +859 967 9355; fax: +859 323 2846.
*E-mail address:* lshlyk@gmail.com (L. Shlyk).

0304-8853/$ - see front matter © 2007 Elsevier B.V. All rights reserved.
doi:10.1016/j.jmmm.2007.04.033

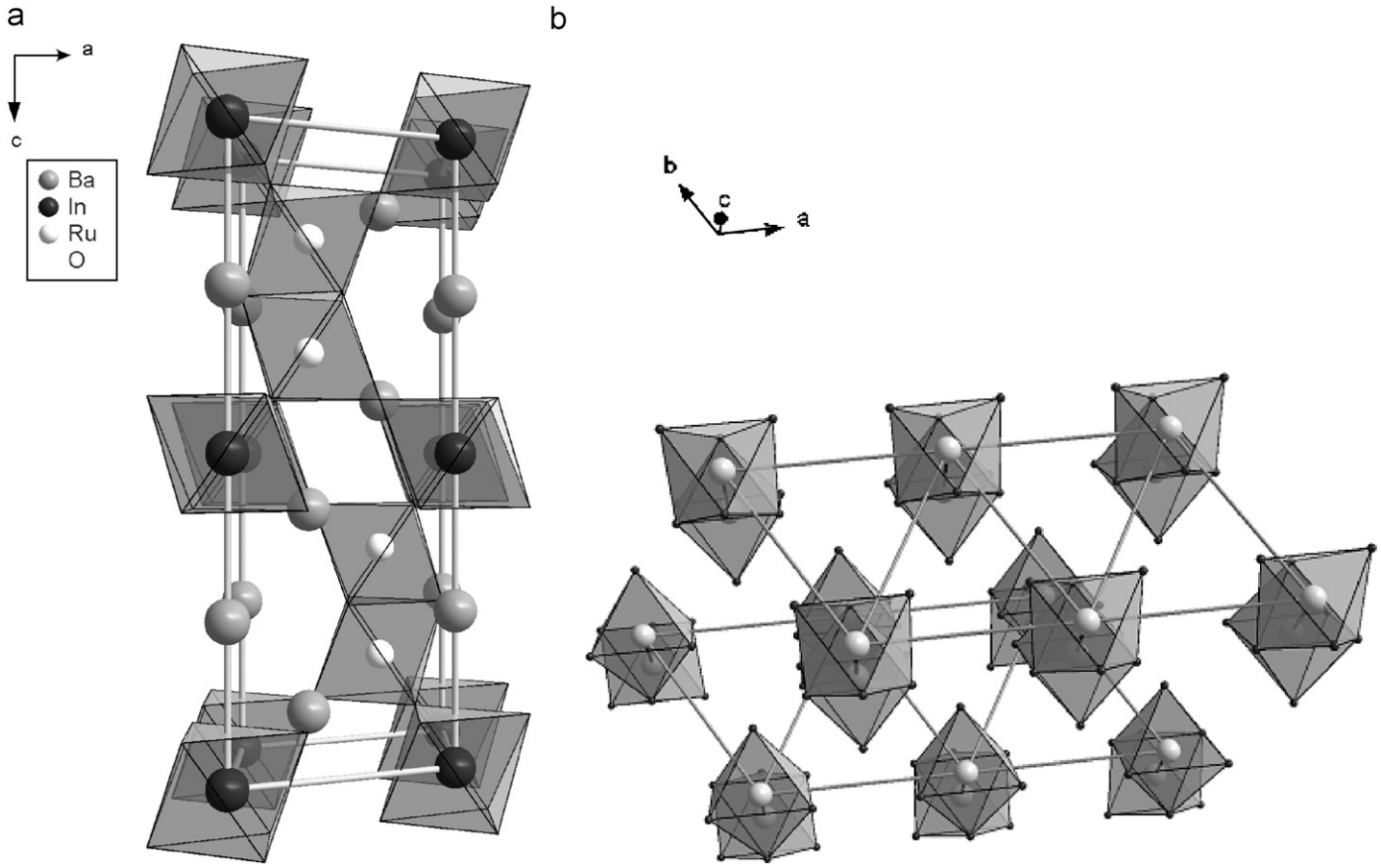


Fig. 1. (a) The unit cell of $Ba_3InRu_2O_9$. (b) The triangular distribution of $Ru_2O_9$ dimers is highlighted by solid lines. The Ba and In atoms have been omitted for clarity.

Table 1
Summary of crystallographic data for a $Ba_3InRu_2O_9$ single crystal

| | |
|---|---|
| Formula | $Ba_3InRu_2O_9$ |
| Formula weight | 879.98 |
| Crystal size | 0.08 mm × 0.05 mm × 0.04 mm |
| Crystal system | Hexagonal |
| Space group | $P6_3/mmc$ |
| Unit cell dimensions | $a = b = 5.8163(1)$Å, $c = 14.3821(5)$Å |
| Volume | 421.252(18)Å |
| $Z$ | 2 |
| Calculated density | 6.881 $Mgm^{-3}$ |
| Absorption coefficient | 20.008 $mm^{-1}$ |
| Scan mode | $\omega$-scans |
| $2\theta$ range (deg) | 0–55° |
| Reflections collected | 8315 |
| Independent reflections | 219 |
| $R_1$ ($I > 2\sigma$(I)) | 2.32% |
| $wR_2$ ($I > 2\sigma$(I)) | 5.02% |
| Goodness of fit | 1.264 |

properties of $Ba_3InRu_2O_9$ using high-quality, single-crystal samples.

## 2. Experimental details

The single crystals were grown by conventional solid-state reaction with excess of $In_2O_3$. The relevant amounts of $BaCO_3$ (99.99%), $RuO_2$ (99.9%) and $In_2O_3$ (99.99%) were weighed and pressed into a pellet. The pellet was placed in an alumina crucible and heated to 1400 °C for ~100 h, after which the sample was slowly cooled to ambient temperature. Single crystals of $Ba_3InRu_2O_9$ (approximate dimensions: 1 mm × 0.5 mm × 0.3 mm) were mechanically extracted from the matrix. X-ray diffraction data were collected at 90.0(2) K on a Nonius Kappa CCD Diffractometer using Mo-K$\alpha$ radiation ($\lambda = 0.71073$ Å). The final full-matrix least-squares refinement converged to $R_1 = 2.32\%$, $wR_2 = 5.02\%$. The crystal structure is illustrated in Fig. 1, and crystallographic data and measurement conditions are summarized in Table 1. Crystal structure and anisotropic displacement parameters are listed in Tables 2 and 3, respectively. The average of

Table 2
Crystal structure parameters of a $Ba_3InRu_2O_9$ single crystal

| Atom | Position | $X$ | $y$ | $z$ |
|---|---|---|---|---|
| Ba1 | 2b | 0 | 0 | 1/4 |
| Ba2 | 4f | 1/3 | 2/3 | 0.91118(6) |
| In1 | 2a | 0 | 0 | 0 |
| Ru1 | 4f | 1/3 | 2/3 | 0.15930(8) |
| O1 | 6h | 0.4867(9) | 0.9734(19) | 1/4 |
| O2 | 12k | 0.1707(6) | 0.3414(13) | 0.4146(4) |

Table 3
Anisotropic displacement parameters, in Å$^2$

| Atom | $U_{11}$ | $U_{22}$ | $U_{33}$ | $U_{12}$ | $U_{13}$ | $U_{23}$ |
|---|---|---|---|---|---|---|
| Ba1 | 0.0056(4) | 0.0056(4) | 0.0058(5) | 0.00279(19) | 0.00000 | 0.00000 |
| Ba2 | 0.0053(3) | 0.0053(3) | 0.0117(4) | 0.00266(16) | 0.00000 | 0.00000 |
| In1 | 0.0042(4) | 0.0042(4) | 0.0034(6) | 0.0021(2) | 0.00000 | 0.00000 |
| Ru1 | 0.0060(4) | 0.0060(4) | 0.0106(5) | 0.0030(2) | 0.00000 | 0.00000 |
| O1 | 0.012(3) | 0.006(4) | 0.019(4) | 0.003(2) | 0.00000 | 0.00000 |
| O2 | 0.011(2) | 0.008(3) | 0.012(2) | 0.0042(15) | 0.0025(14) | 0.005(3) |

Ru–O bond lengths is 1.987 Å. It should be noted that *c*-axis length of a single crystal, 14.3821(5) Å, is considerably larger than that reported for polycrystalline material, 14.3145(7) Å [8]. A possible reason for such difference might be related to the oxygen deficiency in the polycrystalline sample. DC magnetic susceptibility and bulk magnetization were measured using a Quantum Design SQUID Magnetometer in the temperature range of $1.9\,K \leqslant T \leqslant 300\,K$, with magnetic fields $0 \leqslant H \leqslant 5\,T$.

## 3. Results and discussion

The zero-field-cooled (ZFC) and field-cooled (FC) DC susceptibilities are plotted in Fig. 2. The DC susceptibility shows an anomaly for both crystallographic directions at $T_g = 3.5\,K$. There is a distinct anisotropy when the field is applied either parallel or perpendicular to the ab plane. Divergence between ZFC and FC is observed at lower temperatures, typical of spin glasses. The curves show a characteristic plateau in the FC DC susceptibility and a decrease in the ZFC susceptibility below $T_g$, as is usually seen in canonical metallic or insulating spin glasses. The magnetic susceptibility versus temperature increases above ~200 K and does not obey a Curie–Weiss law (Fig. 3). Such magnetic behavior is characteristic for isolated $Ru_2O_9$ dimers and is in good agreement [8] with the results of the magnetic susceptibility previously reported for polycrystalline $Ba_3InRu_2O_9$. The magnetic behavior of polycrystalline samples is attributed to an antiferromagnetic coupling between two Ru ions in a $Ru_2^{4.5+}O_9$ dimer. The magnetization versus magnetic field obtained at $T = 2\,K$ is presented in Fig. 4. It shows nonlinear behavior and does not saturate in a 5 T field. Furthermore, very small hysteresis and remnant magnetization is observed near $H = 0\,T$ (inset in Fig. 4), which is also a characteristic feature of a spin-glass system.

It is advantageous to discuss the magnetic properties in terms of the coordination and packing of the $Ru_2O_9$ octahedra, as it is the Ru ions that are primarily responsible for the magnetic behavior. The structure of $Ba_3InRu_2O_9$ can be considered as consisting from $Ru_2^{4.5+}O_9$ dimers that occupy a hexagonal lattice, as are clearly visible in Fig. 1(b). We suggest that the spin-glass behavior in $Ba_3InRu_2O_9$ can be due to frustration of the dimer magnetic moments on a hexagonal lattice structure. Note that the X-ray structure

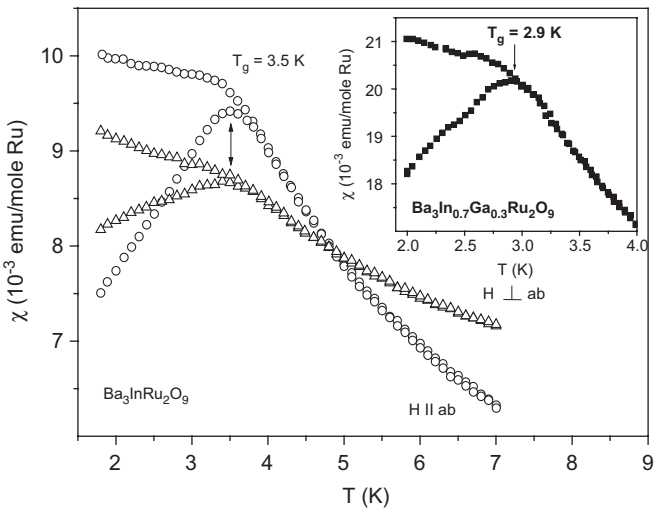


Fig. 2. The FC and ZFC DC susceptibilities of $Ba_3InRu_2O_9$ at and applied field $\mu_oH = 0.01\,T$ for two crystallographic directions. Below $T_g$, the upper curves correspond to FC while the lower curves are for ZFC. The inset shows the FC and ZFC DC susceptibilities of $Ba_3In_{0.7}Ga_{0.3}Ru_2O_9$, which exhibits a slightly depressed spin-glass transition temperature.

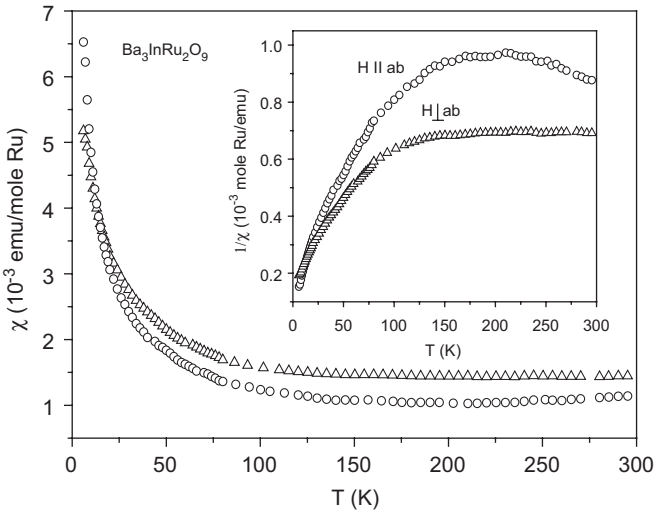


Fig. 3. Temperature dependence of the magnetic susceptibility for $Ba_3InRu_2O_9$ at applied field $\mu_oH = 0.01\,T$. The inset shows the inverse magnetic susceptibility vs. temperature.

refinement is consistent with no site disorder in this compound. Many systems with frustrated lattices do not order above 0 K [9], such as "spin liquids" in which a large fraction of spins remain dynamic down to the lowest temperatures. Special attention is paid to the case of $S = \frac{1}{2}$. That may form quantum spin systems of spin-paired singlets. In the present case of $Ba_3InRu_2O_9$, the $Ru_2^{4.5+}O_9$ dimers consist of $Ru^{4+}$ ($S = 1$) and $Ru^{5+}$ ($S = 3/2$) pairs, which are coupled antiferromagnetically. Therefore, the total spin in the ground state of the dimer is $S = S_1 + S_2 = \frac{1}{2}$, making this system a possible candidate for a spin liquid. However, the spin-glass temperature of $Ba_3InRu_2O_9$ is finite. The observed finite ordering temperature might be explained, for example, by a symmetry-breaking lattice distortion that

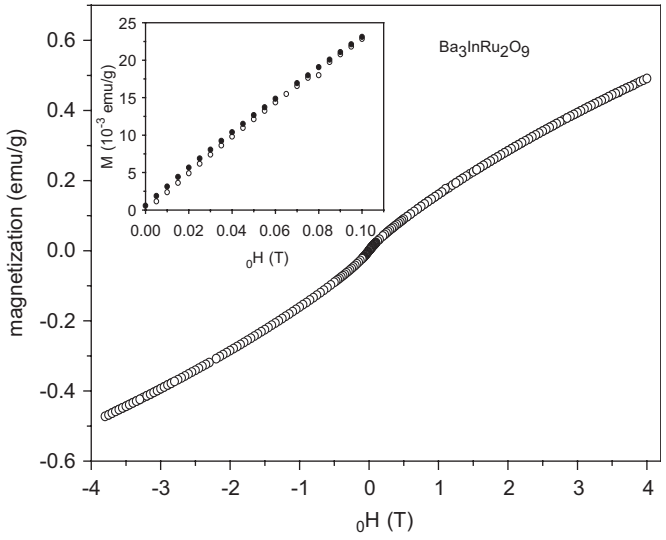


Fig. 4. Magnetization vs. applied field $\mu_o H$ for $Ba_3InRu_2O_9$ at 5 K. The inset shows a small hysteresis at low fields.

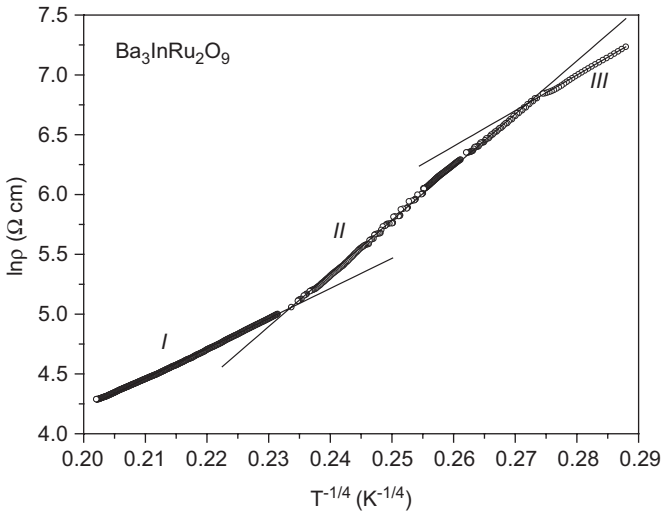


Fig. 5. Temperature dependence of resistivity for $Ba_3InRu_2O_9$ (I||a). The solid lines are fits of the data to Eq. (1) over three separate ranges of temperature.

would alter the exchange parameters and neutralize the frustration. However, it should be noted that the crystal structure at 90 K shows little to no signs of disorder, as the anisotropic displacement parameters all refined to quite reasonable values. Since from the crystal structure it follows that the sublattice of $Ru_2O_9$ dimers is perfectly hexagonal, perhaps there are localized distortions that break the symmetry at close range. In this case, any such distortions would almost certainly be scrambled over the whole crystal and would therefore not change the overall average symmetry. To observe such local distortions, investigations like X-ray-absorption fine-structure (XAFS) are indispensable. At present, these data are not available. On the other hand, we found that the substitution about 30% In by Ga (the $Ga^{3+}$ ionic radius $r_a = 0.62$ Å is smaller than the $In^{3+}$ ionic radius $r_a = 0.8$ Å) has clear impact on the spin-glass transition temperature. The low-temperature magnetic susceptibility of $Ba_3In_{0.7}Ga_{0.3}Ru_2O_9$ is shown in the inset of Fig. 2. It is obvious that the spin-glass transition of $Ba_3In_{0.7}Ga_{0.3}Ru_2O_9$ at $T_g = 2.9$ K is shifted to lower temperatures compared to the pure compound. We speculate that this substitution might partially reduce the local distortions and move $T_g$ to lower temperatures.

The temperature dependence of the resistivity for the single crystal is presented in Fig. 5. This material is nonmetallic, exhibiting increasing resistance with decreasing temperature, which is in agreement with results obtained on polycrystalline samples [5,8]. Generally, the temperature dependence of the resistivity for semiconductors can be described by one of three models: (i) an Arrhenius law for thermally activated behavior; (ii) Mott's variable-range hopping (VRH) expression; and (iii) nearest-neighbor hopping of small polarons. We found that the resistivity can be fitted by Mott's VRH expression, while magnetic-polaron hopping and thermally activated conduction give poorer descriptions. In the VRH model, the conductance of carriers is controlled by the hopping of electrons between local states near the Fermi level. In the case of Mott VRH, the Coulomb interactions among electrons are neglected and the low-temperature resistivity can be expressed as

$$\rho = \rho_0 \exp(T_0/T)^{1/(n+1)}, \quad (1)$$

where $T_0 = 24/\pi L_c^3 N(E_F) k_B$ is the value of the VRH activation energy, $n = 1$, 2 or 3 for one dimensional (1D), 2D or 3D hopping, respectively, and $L_c$ is the localization length and $N(E_F)$ is the density of states at the Fermi level. Fig. 5 indicates that the temperature dependence of the resistivity of a $Ba_3InRu_2O_9$ single crystal follows the relation $\ln\rho \sim T^{-1/4}$ over three distinct temperature ranges including 500–300 K (regime *I*), 320–180 K (regime *II*) and 160–140 K (regime *III*). Fitting the data to Eq. (1), ($n = 3$) yields the VRH activation energy $T_0 \approx 2.4 \times 10^3$ K for regime *I*, $T_0 \approx 2.9 \times 10^3$ K for regime *II* and $T_0 \approx 1.5 \times 10^3$ K for regime *III*. The values of the VRH activation energies are close to the ones observed in other insulating transition metal oxides [10]. Note that there are small but systematic deviations between the fit and the data for the region *II*. Therefore, region *II* might be a crossover regime between regions *I* and *III*. At present, it is difficult to give a clear interpretation for the change in the VRH activation energy with temperature. This will be discussed in a forthcoming paper that reports additional transport and thermodynamic data.

## 4. Conclusion

We have studied magnetic and transport properties of a $Ba_3InRu_2O_9$ single crystal. The magnetic properties of this material at high temperatures can be described in terms of isolated $Ru_2O_9$ dimers. The single crystal displays a spin-glass transition at $T_g = 3.5$ K that is shifted to the lower

temperatures by doping the In sites with ~30%Ga. It is suggested that the magnetic properties at low temperatures are determined by the topology of the $Ru_2^{4.5+}O_9$ dimers, which form a frustrated hexagonal lattice. VRH successfully describes the electrical transport behavior in the temperature range 140–600 K.

## Acknowledgment

This work was in part supported by NSF grant DMR-0552267 and DoE Grant DE-FG02-97IR45653.

## References

[1] Y. Maeno, H. Hashimoto, K. Yoshida, S. Nishizaki, T. Fujita, J.G. Bednorz, F. Lichtenberg, Nature 372 (1994) 532.
[2] G. Cao, S. McCall, M. Shepard, J.E. Crow, R.P. Guertin, Phys. Rev. B 56 (1997) 321.
[3] R.S. Perry, L.M. Galvin, S.A. Grigera, L. Capogna, A.J. Schofield, A.P. Mackenzie, M. Chiao, S.R. Julian, S. Ikeda, S. Nakatsuji, Y. Maeno, C. Pfleiderer, Phys. Rev. Lett. 86 (2001) 2661.
[4] G. Cao, L. Balicas, W.H. Song, Y.P. Sun, Y. Xin, V.A. Bondarenko, J.W. Brill, S. Parkin, X.N. Lin, Phys. Rev. B 68 (2003) 174409; Phys. Rev. B 73 (2006) 224420.
[5] J.T. Rijssenbeek, P. Matl, B. Battlog, N.P. Ong, R.J. Cava, Phys. Rev. B 58 (1998) 10315.
[6] J. Darriert, M. Drillon, G. Villeneuve, Hagenmuller, J. Solid State Chem. 19 (1976) 213.
[7] M. Rath, H.K. Muller-Buschbaum, J. Alloys Compd. 210 (1994) 119.
[8] Y. Doi, K. Matsuhira, Y. Hinatsu, J. Solid State Chem. 165 (2002) 317.
[9] J.E. Greedan, J. Mater. Chem. 11 (2001) 37.
[10] T. Vuletic, B. Korin-Hamzic, S. Tomic, B. Gorshunov, P. Haas, M. Dressel, J. Akimitsu, T. Sasaki, T. Nagata, Phys. Rev. B 67 (2003) 184521.